

ARTICLE OPEN



Pulse oximetry values from 33,080 participants in the Apple Heart & Movement Study

Ian Shapiro¹, Jeff Stein¹, Calum MacRae^{2,3} and Michael O'Reilly¹✉

Wearable devices that include pulse oximetry (SpO₂) sensing afford the opportunity to capture oxygen saturation measurements from large cohorts under naturalistic conditions. We report here a cross-sectional analysis of 72 million SpO₂ values collected from 33,080 individual participants in the Apple Heart and Movement Study, stratified by age, sex, body mass index (BMI), home altitude, and other demographic variables. Measurements aggregated by hour of day into 24-h SpO₂ profiles exhibit similar circadian patterns for all demographic groups, being approximately sinusoidal with nadir near midnight local time, zenith near noon local time, and mean 0.8% lower saturation during overnight hours. Using SpO₂ measurements averaged for each subject into mean nocturnal and daytime SpO₂ values, we employ multivariate ordinary least squares regression to quantify population-level trends according to demographic factors. For the full cohort, regression coefficients obtained from models fit to daytime SpO₂ are in close quantitative agreement with the corresponding values from published reference models for awake arterial oxygen saturation measured under controlled laboratory conditions. Regression models stratified by sex reveal significantly different age- and BMI-dependent SpO₂ trends for females compared with males, although constant terms and regression coefficients for altitude do not differ between sexes. Incorporating categorical variables encoding self-reported race/ethnicity into the full-cohort regression models identifies small but statistically significant differences in daytime SpO₂ (largest coefficient corresponding to 0.13% lower SpO₂, for Hispanic study participants compared to White participants), but no significant differences between groups for nocturnal SpO₂. Additional stratified analysis comparing regression models fit independently to subjects in each race/ethnicity group is suggestive of small differences in age- and sex-dependent trends, but indicates no significant difference in constant terms between any race/ethnicity groups for either daytime or nocturnal SpO₂. The large diverse study population and study design employing automated background SpO₂ measurements spanning the full 24-h circadian cycle enables the establishment of healthy population reference trends outside of clinical settings.

npj Digital Medicine (2023)6:134; <https://doi.org/10.1038/s41746-023-00851-6>

INTRODUCTION

Arterial blood oxygen saturation (SaO₂) is the fraction of hemoglobin containing bound oxygen relative to the total functional hemoglobin, and represents a key parameter indicative of cardiopulmonary function. Direct SaO₂ measurement necessitates an invasive arterial blood draw and blood gas analysis. Pulse oximetry enables non-invasive measurement of blood oxygen saturation (SpO₂) and provides a convenient estimate of SaO₂ that does not require arterial blood removal. The SpO₂ measurement relies upon quantifying changes in optical attenuation at two separate wavelengths (typically one red and one infrared), with signal content arising from pulsatile arterial blood modulation in response to individual heartbeats. Depending on design, pulse oximeters may operate in either transmissive mode, with the interrogating light propagating across a thin section of capillary rich tissue (commonly fingertip, earlobe, or toe), or in reflectance mode wherein the interrogating light scatters back in the direction of the optical illuminator. Reflectance SpO₂ is employed by consumer smart watch devices such as the Apple Watch (selected models) as well as selected products from Fitbit, Garmin, Samsung, Withings, and other manufacturers.

Oxygen saturation determined from SaO₂ or SpO₂ is often considered a “fifth vital sign” due to its relative ease of capture and high clinical utility^{1,2}. As a physiological metric, arterial oxygen saturation directly impacts systemic oxygen delivery in

conjunction with cardiac output and hemoglobin concentration. Among healthy awake individuals, typical SpO₂ values lie in the range of 95–99%. Low blood oxygen saturation can arise from impaired lung function (e.g., reduced diffusion capacity), ventilation-perfusion mismatch, cardiac shunt, low cardiac output, or low oxygen concentration in the inspired air (e.g., due to altitude). No single universal SpO₂ threshold is applied in all medical use cases, but values less than 92% from individuals breathing room air at sea level generally prompt further investigation, with values remaining persistently below 90% indicating hypoxemia. Oxygen saturation is utilized to guide management of cardiopulmonary conditions such as chronic obstructive pulmonary disease (COPD), obesity hypoventilation syndrome (OHS), and obstructive sleep apnea (OSA).

Cross-sectional studies involving single-setting SpO₂ or SaO₂ measurements from nominally healthy individuals at constant altitude have consistently reported negative correlation of blood oxygen saturation with both age and body mass^{3–7}. Studies incorporating multiple altitudes or a range of barometric pressure consistently report a positive linear relationship between awake arterial oxygen saturation and barometric pressure, in agreement with expectations based on the alveolar gas equation^{3,8,9}. Less consistently, some studies have also reported positive correlation between SpO₂ and female sex^{5,10,11}, although others have reported negative or insignificant SpO₂ findings with respect to

¹Apple Inc., Cupertino, CA, USA. ²Cardiovascular Medicine Division, Brigham and Women's Hospital, Boston, MA, USA. ³Harvard Medical School, Boston, MA, USA. ✉email: mor@apple.com

sex¹². A similar mix of conclusions has been published with respect to tobacco smoking status, with some studies reporting lower SpO₂ values for current smokers⁶ and others reporting no significant relationship⁵.

In the context of clinical screening and risk estimation for chronic cardiopulmonary disease, single-point SpO₂ measurements below 95% saturation have been reported as predictive of a variety of cardiopulmonary conditions and outcomes^{13–18}. The Tromsø Study examined single-event SpO₂ values and 10-year outcomes for cardiopulmonary disease, reporting significant elevated risk for values $\leq 92\%$ and 93–95% saturation, compared with 96–100% saturation¹⁴. Daytime SpO₂ has been reported as a significant independent predictor of hypertension¹³, as well as circulatory impairment in the form of impaired left ventricular filling¹⁵. Mean overnight SpO₂ has also been reported as predictive of both absolute waking blood pressure and magnitude of morning blood pressure surge¹⁶. Studies examining overnight SpO₂ in the context of atherosclerotic cardiovascular risk have produced inconsistent findings, with some reporting significant relationships between mean overnight SpO₂ and presence of carotid artery plaque¹⁷, and others reporting no significant relationship after adjusting for demographic variables and other known risk factors¹⁸.

In the present study we analyze systematic variation in mean daytime and nocturnal SpO₂ captured by wearable devices, stratified by age, gender, body mass index (BMI), home altitude, and other self-identified demographic factors including race and ethnicity. All subject groups exhibit approximately sinusoidal variation in mean SpO₂, with highest values in mid-day and mean 0.8% lower saturation during nocturnal hours compared to daytime hours. We employ linear regression models to quantify these trends and enable comparison with existing published reference equations developed from smaller studies utilizing

arterial blood gas analysis^{3,19} and pulse oximetry²⁰. Both daytime SpO₂ and nocturnal SpO₂ exhibit a progressive decline with increasing age, BMI and home altitude. Compared with daytime SpO₂, nocturnal SpO₂ regression models yielded higher coefficients of determination and emphasize the effects of age, BMI, and altitude in all subject groups. Additionally, the large subject pool in this study enables us to detect small but significant differences in age- and BMI-dependent trends in SpO₂ between sexes, with female subjects displaying a greater rate of age-dependent decline in both daytime SpO₂ and nocturnal SpO₂.

RESULTS

Population distributions of mean daytime and nocturnal SpO₂

Figure 1 shows 24-h SpO₂ profiles (mean \pm 99.5% confidence interval) stratified by decade of age, BMI group, gender, and location-inferred home altitude. All subject groups exhibited systematic 24-h variation in SpO₂ with lowest mean values occurring during nocturnal hours (nadir approximately 01:00 local time), and highest mean values occurring during mid-day hours (zenith approximately 11:00). The general cohort (Fig. 2) exhibited a mean diurnal range of approximately 1% saturation. Subject groups having lower mean daytime SpO₂ tended to yield a larger mean 24-h range of SpO₂ and disproportionately lower nocturnal SpO₂, examples of which can be observed for older subject groups (Fig. 1a) and for subjects residing at >1000 m altitude (Fig. 1c).

Daytime and nocturnal SpO₂ variation with subject age, BMI, and home altitude

Histograms of dSpO₂ and nSpO₂ are shown in Fig. 3. In the full cohort, mean dSpO₂ was 96.17 [SD 1.28]%; mean nSpO₂ was 95.38 [SD 1.47]%; and mean dn Δ SpO₂ was 0.78 [SD 0.98]%. Both dSpO₂

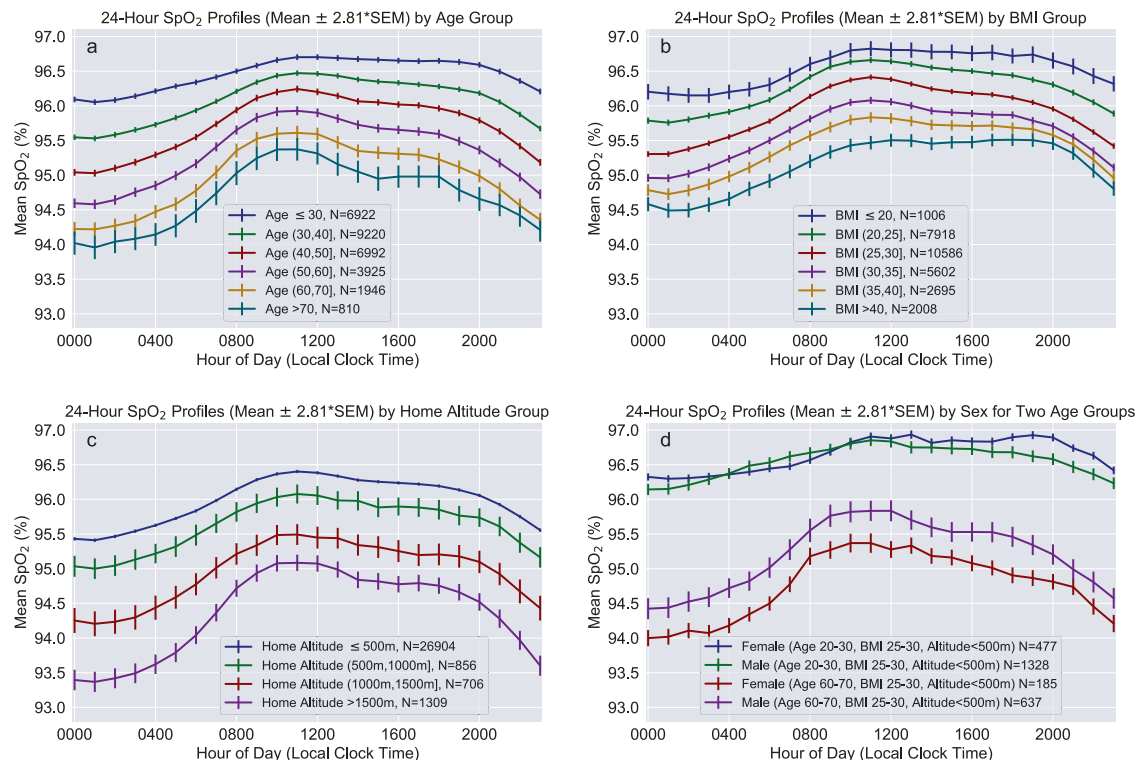


Fig. 1 Twenty-four-hour group mean SpO₂ profiles stratified by demographic variables and home altitude. Profiles are stratified according to **a** age, **b** body mass index, **c** home altitude and **d** assigned sex for two age groups with limited range of BMI and home altitude. Solid lines indicate group mean value for each hour, with whiskers indicating ± 2.81 times the SEM (equivalent to 99.5% confidence interval for the mean value) for each hour. Group profiles were determined by first generating the hourly SpO₂ profile for each subject, then calculating the mean and SEM across subjects for each hour as described in the “Methods” section. SEM standard error of the mean.

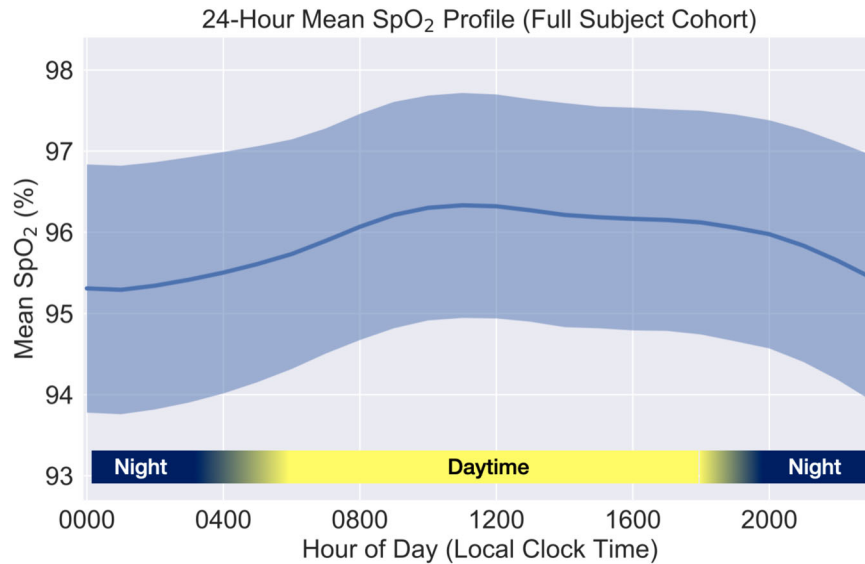


Fig. 2 Twenty-four-hour SpO₂ variation for the full study cohort, shown as the mean \pm standard deviation after subject-level hourly profile aggregation as described in the “Methods” section.

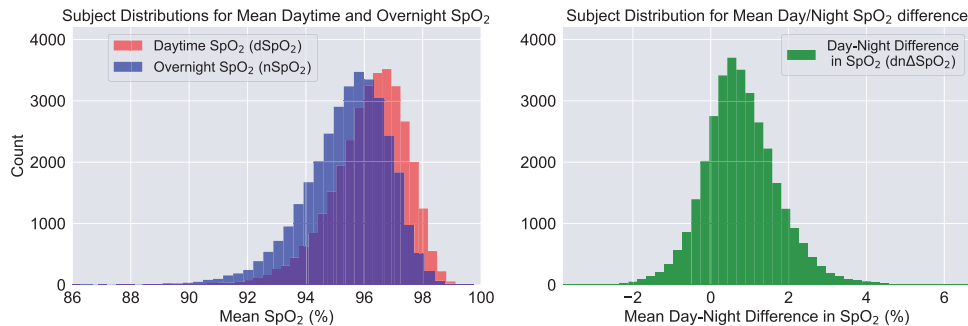


Fig. 3 Population distributions of measured mean oxygen saturation values. Separate distributions are shown for daytime mean saturation (dSpO₂, left panel), nocturnal mean saturation (nSpO₂, left panel) and mean day-night SpO₂ difference (dn Δ SpO₂, right panel) for the full study cohort. Positive values for dn Δ SpO₂ correspond to lower measured SpO₂ at night.

and nSpO₂ were significantly correlated with age, BMI, and altitude, and exhibited a monotonic decreasing trend with each of these variables. Figure 4 shows 2D histograms for these metrics overlaid with the corresponding univariate linear regression line, slope and Pearson correlation coefficient. In all cases, both the absolute slope and the correlation coefficients were greater for nSpO₂ than for dSpO₂. For daytime SpO₂, measured slopes with respect to each of these variables were in good quantitative agreement with existing publications^{3,8,9}. Table 1 compares the slopes and intercepts for simple univariate regression of daytime SpO₂ using only age as the independent variable (for subjects with home altitude below the study median of 155m) with the equivalent low-altitude univariate model reported by Crapo et al.³.

Linear regression results for model M_{Ref} fit to both daytime and nocturnal SpO₂ using the full subject cohort are summarized and compared with the reference results reported by Crapo et al. in Table 2. For daytime SpO₂ the fitted constant term (89.25%, 99.5% CI 88.68–89.83) differs by less than 0.2% saturation compared with the constant term from the reference SaO₂ model. The value of this constant term is not physiologically interpretable as it corresponds to the predicted oxygen saturation at zero age, weight, and barometric pressure, but instead provides an indication of absolute calibration agreement between the SaO₂ and SpO₂ sensors used by the two studies. For daytime SpO₂ the model coefficients for age, weight, and barometric pressure all have 5–20% smaller absolute magnitude compared with the

corresponding reference model coefficients. In contrast, for nocturnal SpO₂ the fitted model coefficients have 5–20% greater magnitude compared with reference model coefficients. Additionally, on our data set the nocturnal SpO₂ model fit yields a statistically significant term for sex (0.16% higher nSpO₂ for males, 99.5% CI 0.11–0.22, $p = 2.7 \times 10^{-16}$), and both daytime and nocturnal SpO₂ model fits yield statistically significant coefficients for height, in contrast to the published reference SaO₂ model which did not report significant fit coefficients for sex or height.

Linear regression results for model M_1 fit to the full subject cohort for dSpO₂ and nSpO₂ are listed in Table 3. For both dSpO₂ and nSpO₂, all M_1 regression coefficients for age, BMI, and home altitude are highly significant. For nocturnal SpO₂, no coefficients corresponding to categorical variables were identified as significant. However, M_1 fit using daytime SpO₂ produced significant coefficient for sex (0.05% higher SpO₂ for females, 99.5% CI 0.01–0.09, $p = 4.1 \times 10^{-4}$), Asian race/ethnicity compared with White race/ethnicity (0.10% higher SpO₂ for White participants, 99.5% CI 0.03–0.17, $p = 1.2 \times 10^{-4}$), and for Hispanic race/ethnicity compared with White race/ethnicity (0.13% higher SpO₂ for White participants, 99.5% CI 0.07–0.19, $p = 4.8 \times 10^{-10}$).

Regression models stratified by sex and race/ethnicity

For the purposes of sex-specific stratified analysis, we compared $M_{1,sex}$ models fit for male and female subjects separately with M_1 models fit for full cohort. The fitted model coefficients and

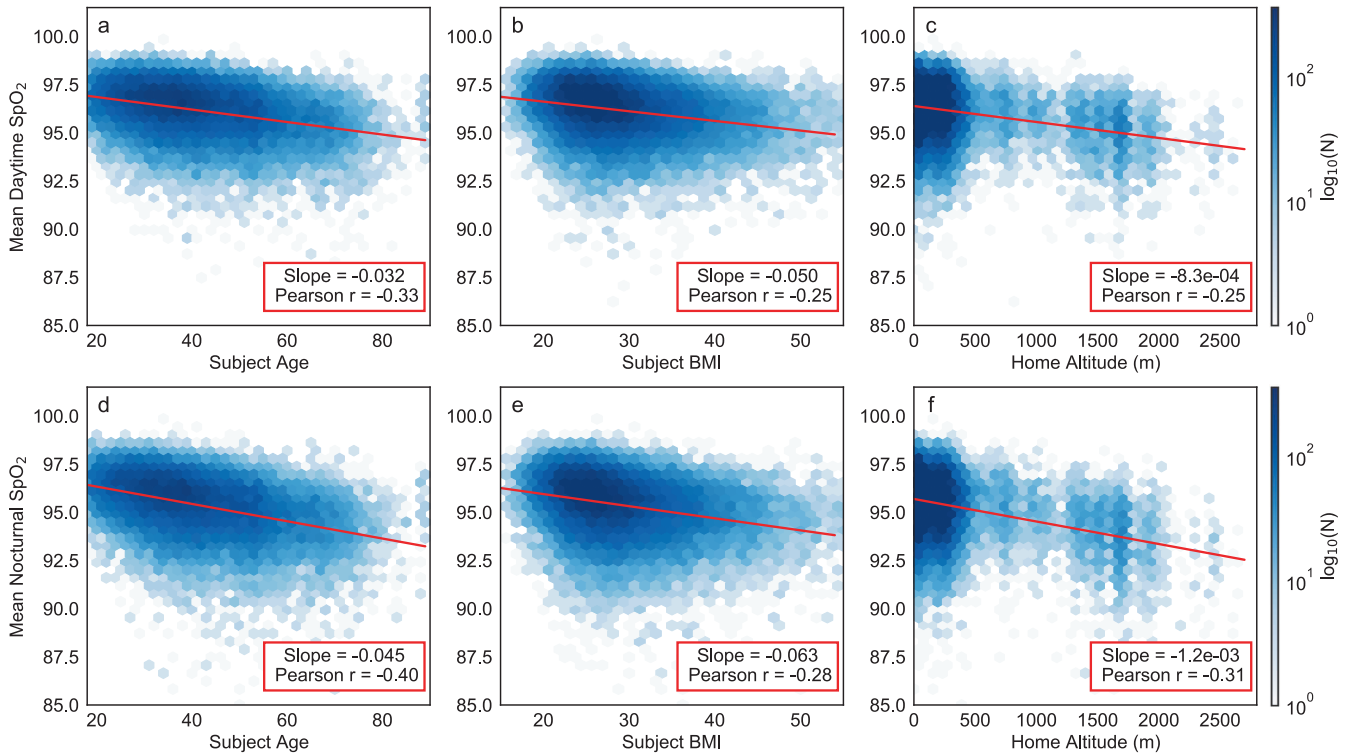


Fig. 4 Linear relationships between measured mean oxygen saturation values and each of three independent variables exhibiting the strongest correlation with these metrics. **a–c** (top row) correspond to mean daytime SpO₂. **d–f** (bottom row) correspond to mean nocturnal SpO₂. Independent variables consist of: **a, d** age, **b, e** body mass index, **c, f** home altitude. Each plot presents a 2-dimensional histogram of values from all 33,080 subjects in evenly spaced hexagonal bins, with the color density corresponding to log-scaled bin counts for visual clarity. In each plot, the overlaid red line represents the simple univariate linear regression fit using the independent variable shown on the x-axis. The listed slope and Pearson correlation coefficient correspond to the same univariate linear fit.

Table 1. Tabulated comparison of reference SaO₂ linear model coefficients (top row of coefficients; adapted from ref. ³) with results obtained from equivalent fits to daytime mean SpO₂ (bottom row of coefficients) using only low-altitude subjects (estimated home altitude < 155m) from our data set.

Univariate regression results for blood oxygen saturation (low-altitude subjects only)				
Model	R ²	SEE	Constant	Age (years)
Reference univariate SaO ₂ (Crapo et al. ³)	0.32	0.85	97.66	-0.0296
Daytime SpO ₂ (low-alt. subjects)	0.12	1.14	97.65 (97.57, 97.74) [p < 1.0e-10]	-0.0322 (-0.0341, -0.0303) [p < 1.0e-10]

Values in parentheses indicate 99.5% confidence intervals for fit coefficients. Values in brackets are regression coefficient *p* values, corresponding to two-sided *t* tests under the null hypothesis that the coefficient is equal to zero. R² coefficient of determination, SEE standard error of the estimate.

confidence intervals are plotted in Fig. 5 to facilitate visual comparison, with the results also tabulated in Supplementary Table 5. For both sexes as well as the full subject cohort, coefficients of determination (R²) were higher for models fit to nSpO₂ compared with dSpO₂. Additionally the fitted model coefficients for age, BMI, and altitude variables all exhibited significantly larger absolute magnitudes for nSpO₂ compared to dSpO₂ (implying a greater impact on SpO₂ from each of these variables at night). This phenomenon of greater impact on SpO₂ from each of these variables overnight is also observable in the grouped 24-h mean profiles shown in Fig. 1a–c, in which the separation between stratified 24-h profiles is consistently larger during nocturnal hours.

Comparing female- and male-specific models shows no meaningful differences for constant terms and altitude coefficients between sexes, in either dSpO₂ models (Fig. 5a, d) or nSpO₂ models (Fig. 5e, h). However, the coefficients for age differ

significantly between the sex-specific models for both dSpO₂ ($p = 1.4 \times 10^{-24}$, Fig. 5b) and nSpO₂ ($p = 4.5 \times 10^{-18}$, Fig. 5f), with females producing a larger magnitude for age coefficients (implying greater decline in SpO₂ with age) for both measurement periods. Additionally, BMI coefficients also differ significantly between sex-specific models for both dSpO₂ ($p = 1.1 \times 10^{-3}$, Fig. 5c) and nSpO₂ ($p = 1.9 \times 10^{-10}$, Fig. 5g), with males producing a larger coefficient magnitude (implying greater decline in SpO₂ with increasing BMI).

For additional subgroup analysis we fit model $M_{1, race-ethn}$, separately for subjects in each of the five race/ethnicity groups reported in the study demographics (Table 4). All race/ethnicity subgroup regression results are plotted in Fig. 6 to facilitate visual comparison, with results tabulated in Supplementary Table 6. Comparing regression coefficients between subgroup models using Welch's unequal variances *t* test, and employing the Bonferroni-corrected *p* value threshold of 0.0005 to determine

Table 2. Tabulated comparison of reference SaO₂ linear model coefficients (top row of coefficients; adapted from reference³) with linear model coefficients obtained from equivalent fits to daytime mean SpO₂ (middle row of coefficients) and overnight SpO₂ (bottom row of coefficients) using our data.

Linear regression results for blood oxygen saturation: fit coefficients for reference model (M_{ref})										
Model	R^2	SEE	Constant	Age (years)	Baro. Press. (mm Hg)	Weight (kg)	Sex ($m = 1, f = 0$)	Height (cm)		
Reference SaO ₂ (Crapo et al. ³)	0.56	0.85	89.41	-0.0362	0.0128	-0.0159	n.s.	n.s.		
Daytime SpO ₂	0.23	1.13	89.25 (88.68, 89.83) [$p < 1.0e-10$]	-0.0309 (-0.0322, -0.0296) [$p < 1.0e-10$]	0.0100 (0.0094, 0.0105) [$p < 1.0e-10$]	-0.0149 (-0.0157, -0.0140) [$p < 1.0e-10$]	-0.0168 (-0.0686, 0.0351) [$p = 0.36$]	0.0123 (0.0098, 0.0149) [$p < 1.0e-10$]		
Nocturnal SpO ₂	0.32	1.21	87.12 (86.50, 87.74) [$p < 1.0e-10$]	-0.0431 (-0.0445, -0.0417) [$p < 1.0e-10$]	0.0140 (0.0134, 0.0146) [$p < 1.0e-10$]	-0.0182 (-0.0192, -0.0173) [$p < 1.0e-10$]	0.1629 (0.1071, 0.2187) [$p < 1.0e-10$]	0.0069 (0.0042, 0.0097) [$p < 1.0e-10$]		

Values in parentheses indicate 99.5% confidence intervals for fit coefficients. Values in brackets are regression coefficient p values, corresponding to two-sided t tests under the null hypothesis that the coefficient is equal to zero.

R^2 coefficient of determination, SEE standard error of the estimate, n.s. not significant.

Table 3. Linear model M_1 full-cohort fit results for daytime SpO₂ (top row of coefficients) and nocturnal SpO₂ (bottom row of coefficients).

Linear regression results for proposed model (M_1)											
Model	R^2	SEE	Constant	Age (years)	BMI (kg/m ²)	Altitude (km)	Sex ($m = 1, f = 0$)	Asian race/ethnicity	Black race/ethnicity	Hispanic race/ethnicity	Other race/ethnicity
Full-cohort daytime SpO ₂	0.23	1.12	96.66 (96.62, 96.70) [$p < 1e-10$]	-0.0314 (-0.0327, -0.0300) [$p < 1e-10$]	-0.0457 (-0.0484, -0.0430) [$p < 1e-10$]	-0.8402 (-0.8845, -0.7959) [$p < 1e-10$]	-0.0490 (-0.0880, -0.0101) [$p = 4.1e-04$]	-0.1004 (-0.1735, -0.0273) [$p = 1.2e-04$]	-0.0648 (-0.1446, 0.0150) [$p = 0.023$]	-0.1334 (-0.1936, -0.0733) [$p = 4.8e-10$]	-0.0146 (-0.0986, 0.0694) [$p = 0.63$]
Full-cohort nocturnal SpO ₂	0.32	1.21	95.95 (95.91, 95.99) [$p < 1e-10$]	-0.0429 (-0.0444, -0.0415) [$p < 1e-10$]	-0.0562 (-0.0591, -0.0533) [$p < 1e-10$]	-1.1736 (-1.2214, -1.1257) [$p < 1e-10$]	-0.0038 (-0.0459, 0.0775) [$p = 0.80$]	0.0775 (-0.0015, 0.1564) [$p = 0.0059$]	-0.0068 (-0.0930, 0.0794) [$p = 0.82$]	0.0243 (-0.0406, 0.0893) [$p = 0.29$]	0.0596 (-0.0311, 0.1504) [$p = 0.065$]

Sex variables for the full subject cohort are encoded using a value of 1 for male subjects and 0 for female subjects. Race/ethnicity variables for the full cohort and both sexes encoded using a value of 1 for each listed race/ethnicity group, with White subjects encoded using all zeros. Values listed in parentheses represent 99.5% confidence intervals for the fitted model coefficients. Values in brackets are regression coefficient p values, corresponding to two-sided t tests under the null hypothesis that the coefficient is equal to zero.

R^2 coefficient of determination, SEE standard error of the estimate.

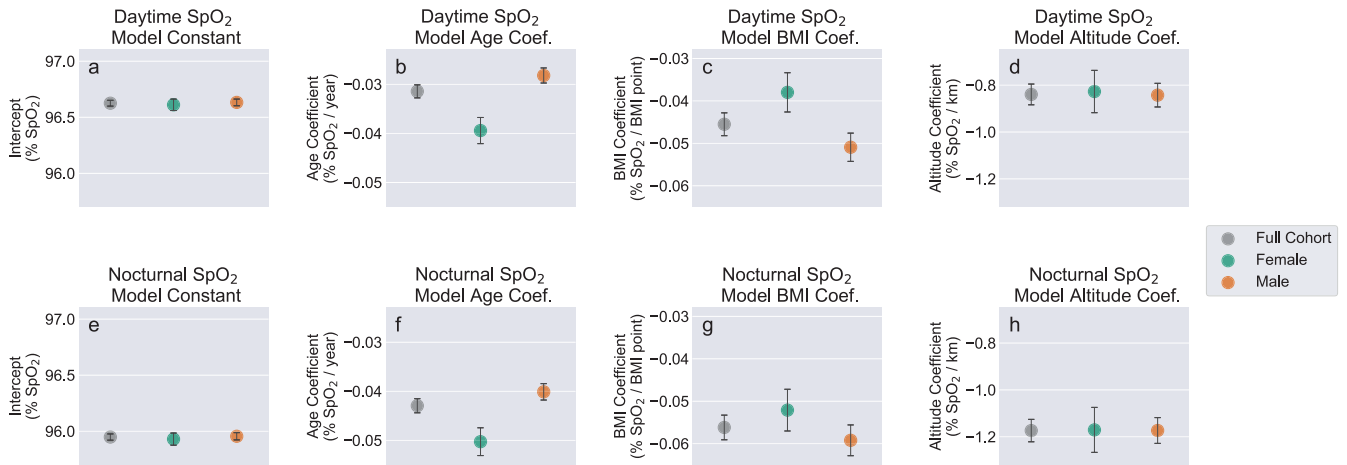


Fig. 5 Comparison of fit coefficients for M_1 models fit to the full cohort and $M_{1,sex}$ models fit independently to female and male subjects. **a–d** (top row) correspond to models fit using mean daytime SpO_2 . **e–h** (bottom row) correspond to models fit using mean nocturnal SpO_2 . Regression coefficients consist of: **a, e** constant term, **b, f** age, **c, g** body mass index, **d, h** home altitude. Error bars represent 99.5% confidence intervals for the fitted coefficients. Race/ethnicity variables are omitted for clarity. Plotted coefficients and confidence intervals are identical to the values listed in Supplementary Table 5.

statistical significance, identified the following significant pairwise coefficient differences (p values for significance tests are shown; individual coefficient values and confidence intervals are listed in Supplementary Table 6):

- Age coefficients (daytime SpO_2): Significant group differences for Asian participants compared with Other participants ($p = 4.7 \times 10^{-6}$), and for Asian compared with White participants ($p = 3.7 \times 10^{-6}$).
- Age coefficients (nocturnal SpO_2): Significant group differences for Asian compared with Hispanic participants ($p = 7.6 \times 10^{-6}$), for Asian compared with Other participants ($p = 2.7 \times 10^{-7}$), and for Asian compared with White participants ($p = 9.2 \times 10^{-8}$).
- Altitude coefficients (nocturnal SpO_2): Significant group differences for Hispanic compared with Other participants ($p = 1.6 \times 10^{-4}$), and for Hispanic compared with White participants ($p = 2.4 \times 10^{-4}$).
- Sex coefficients (daytime SpO_2): Significant group differences for Asian compared with Black participants ($p = 2.8 \times 10^{-5}$), and for Black compared with White participants ($p = 3.0 \times 10^{-7}$).
- Sex coefficients (nocturnal SpO_2): Significant group differences for Asian compared with Black participants ($p = 3.8 \times 10^{-4}$).

All other pairwise group comparisons, including all comparisons for constant terms and BMI coefficients, were not determined to be significant.

DISCUSSION

All subject groups in our data set exhibited diurnal variation with similar circadian profiles, consisting of nadir during typical overnight sleep hours and zenith in mid-day (Figs. 1 and 2). Few prior studies have examined systematic 24-h circadian variation in oxygen saturation for healthy adult individuals under naturalistic conditions. Existing studies examining overnight SpO_2 compared with daytime awake SpO_2 have typically focused on cohorts presenting with a chronic cardiopulmonary disease such as COPD or sleep apnea. However, findings reported in existing publications regarding circadian and diurnal variation in blood oxygen saturation are in general agreement with both the scale and phase of SpO_2 variation observed in our data set. A study of 77 healthy pediatric subjects from whom SpO_2 values were collected at 2-h cadence for 24 h reported systematic sinusoidal variation having

an average amplitude of 2% saturation, with lowest values during mid-sleep and highest values in early afternoon hours²¹. Similarly, a study of diurnal variation in arterial oxygen saturation among 22 healthy young adult individuals (mean age 20 years) living at 2600m altitude found that lowest values consistently occurred between hours 01:00 and 03:00²². Circadian variation independent of sleep status has also been reported for pulmonary function metrics measured from healthy subjects under controlled conditions, with lowest measured pulmonary function occurring typical sleep hours even while subjects remained awake^{23,24}. Combined with prior studies of both healthy individuals and individuals with chronic pulmonary disease which reported no significant differences arterial oxygen pressures for sitting vs. standing and supine positions²⁵, this suggests that the lower mean SpO_2 observed during nocturnal hours is driven primarily by endogenous variation in cardiopulmonary parameters in concert with sleep/wake cycle, rather than by typical recumbent body positions during sleep.

For linear regression models fit to the full subject cohort and for specific subject groups (Table 3 and Supplementary Tables 5 and 6) we have measured consistently stronger effects from age, BMI, and altitude (as well as higher coefficients of determination) for nocturnal SpO_2 values compared with daytime SpO_2 values. These phenomena are not specific to the two time windows we have chosen to define daytime and nocturnal measurement periods, but occur consistently for clock hours typically associated with sleep vs. waking and transitional periods (illustrated in Supplementary Fig. 3). The larger effect size at night for these systematic drivers of SpO_2 , combined with the superior model fits for nocturnal SpO_2 , suggests that sleeping conditions provide the best opportunity to resolve meaningful physiological differences as well as avoid potential confounds due to daytime behavior.

Additionally, as can be observed in 24-h mean SpO_2 profiles for various cohorts (Fig. 1), subgroups with lower daytime SpO_2 also tend to exhibit a greater decline in SpO_2 during overnight hours. The three independent variables that most strongly influence daytime and nocturnal SpO_2 (age, BMI, and altitude) are also significant predictors of the change in SpO_2 from day to night ($dn\Delta SpO_2$). The correlation between $dn\Delta SpO_2$ and these three independent variables is illustrated in Supplementary Fig. 6. Identifying and quantifying additional unexplained factors driving systematic nocturnal changes in SpO_2 (specifically instances with overnight decline) merits further investigation.

Table 4. Summary of dataset statistics for the full cohort and demographic groups used for stratified and subgroup analysis.

Subject group	N (%)	Age, years (mean ± std. dev.)	BMI, kg/m ² (mean ± std. dev.)	Home altitude, m (mean ± std. dev.)	Daytime SpO ₂ , % (mean ± std. dev.)	Nocturnal SpO ₂ , % (mean ± std. dev.)
Full cohort	33,080 (100.0%)	41.0 ± 13.2	28.9 ± 6.5	260.4 ± 392.9	96.2 ± 1.3	95.4 ± 1.3
Female assigned sex	9169 (27.7%)	40.3 ± 13.1	29.5 ± 7.6	268.6 ± 384.7	96.2 ± 1.4	95.4 ± 1.4
Male assigned sex	23,911 (72.3%)	41.3 ± 13.2	28.7 ± 6.1	257.3 ± 395.9	96.2 ± 1.3	95.4 ± 1.3
Asian race/ethnicity	2063 (6.2%)	37.8 ± 11.8	26.3 ± 4.8	179.2 ± 309.6	96.4 ± 1.2	95.8 ± 1.2
Black race/ethnicity	1687 (5.1%)	39.4 ± 11.8	30.8 ± 7.3	198.3 ± 311.6	96.2 ± 1.3	95.4 ± 1.3
Hispanic race/ethnicity	3162 (9.6%)	36.9 ± 11.1	29.6 ± 6.6	254.9 ± 410.6	96.2 ± 1.3	95.5 ± 1.3
Other race/ethnicity	1501 (4.5%)	39.9 ± 12.0	29.3 ± 6.8	244.1 ± 366.6	96.2 ± 1.4	95.5 ± 1.4
White race/ethnicity	24,667 (74.6%)	42.0 ± 13.5	28.8 ± 6.5	273.2 ± 401.9	96.2 ± 1.3	95.3 ± 1.3

The age-dependent average decline in oxygen saturation measured for the full subject cohort ($-0.031\%/year$ for $dSpO_2$) is in close quantitative agreement with trends published previously by other researchers ($-0.036\%/year$ reported by Crapo et al.³, $-0.027\%/year$ reported by Perez-Padilla et al.²⁰, $-0.020\%/year$ reported by Klæstrup, et al.¹⁹). Progressive decline in pulmonary function with age has been described extensively in research literature, with quantitative trends reported for spirometry metrics, respiratory muscle function, gas exchange metrics, and physical lung tissue properties such as elastic recoil and alveolar size²⁶. Age-related lung tissue changes include progressive remodeling of the collagen fibers that surround and support the alveoli, contributing to increased average alveolar size and loss of elastic recoil. Combined, this results in a tendency for smaller airways of older lungs to close during breathing even under resting conditions²⁷. The closure of these airways translates into mismatch between alveolar ventilation and pulmonary capillary perfusion (V/Q mismatch) which hampers the diffusion of inhaled oxygen into the arterial blood stream²⁸. Additionally, alveolar enlargement reduces total alveolar surface area, which further impairs gas exchange and contributes to increasing alveolar-arterial O₂ gradient²⁶. Collectively these age-related changes cause a progressive decline in arterial oxygen saturation that is approximately linear with age, even in the absence of overt lung disease^{3,19,29}.

Our findings regarding the continuous linear relationship between increasing body weight and decreasing arterial oxygen saturation (measurable even between non-obese BMI categories) is in close quantitative agreement with prior published work. The linear regression model for daytime SpO₂ fit to the full subject cohort in our data set (Table 3) yields a slope of $-0.046\%/BMI$ -point for $dSpO_2$, compared with $-0.036\%/BMI$ -point reported by Perez-Padilla et al.²⁰.

Body weight-associated changes in pulmonary function and arterial oxygen saturation have been studied most commonly in the context of severe obesity (BMI > 40)^{30–33}, although some published research has reported significant trends in spirometry metrics as a function of BMI even for normal and overweight (non-obese) categories^{34–37}. Researchers have consistently reported a negative correlation between arterial oxygen saturation and BMI or weight, even in the absence of obstruction or pulmonary comorbidities. The hypothesized mechanisms of interaction between body composition and pulmonary function include both direct mechanical effects such as lung unit closure and atelectasis (reducing functional lung capacity, and increasing V/Q mismatch), as well as adiposity-mediated pulmonary tissue inflammation^{38,39}. Further, these obesity-related effects on pulmonary function and oxygen saturation are expected to have a greater impact during nocturnal sleep hours compared with awake daytime hours⁴⁰, which may explain the slightly larger effect size for BMI we have measured for $nSpO_2$ vs. $dSpO_2$ in the full cohort and all subject groups ($-0.046\%/BMI$ -point for $dSpO_2$ vs. $-0.056\%/BMI$ -point for $nSpO_2$ fit using the full subject cohort).

The sex-specific regression models (summarized in Fig. 5 and Supplementary Table 5) support two conclusions regarding systematic differences in SpO₂ trends between sexes. First, SpO₂ tends to decline more rapidly with increasing BMI for males than females. Additionally, SpO₂ tends to decline more rapidly with increasing age for females than males. Although some existing blood oxygen saturation studies have reported small but significant relationships between measured SpO₂ and female sex (exclusively as additive sex-specific offsets^{5,10,11}), to our knowledge no prior published work has quantified differing sex-dependent trends for age and BMI.

The sex-specific difference in SpO₂ trend vs. BMI (Fig. 5c) may be attributable to systematic variation in body fat distribution between males and females. Males tend to have disproportionately higher abdominal and visceral adipose tissue than females,

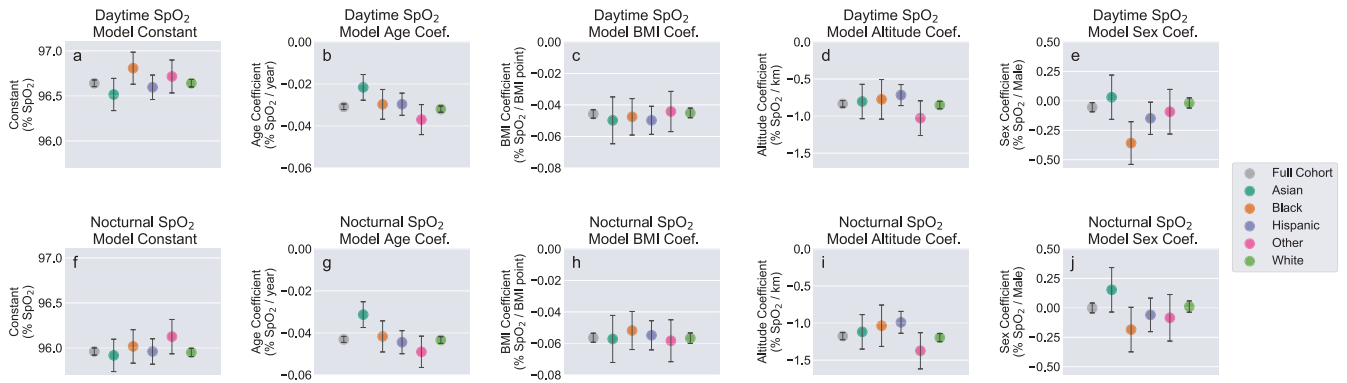


Fig. 6 Comparison of model coefficients for for M_1 models fit to the full cohort, and for $M_{1,race-ethn.}$ models fit independently to each race/ethnicity group. **a–e** (top row) correspond to models fit using mean daytime SpO_2 . **f–j** (bottom row) correspond to models fit using mean nocturnal SpO_2 . Regression coefficients consist of: **a, f** constant term, **b, g** age, **c, h** body mass index, **d, i** home altitude, **e, j** assigned sex. Error bars represent 99.5% confidence intervals for the fitted coefficients. Plotted coefficients and confidence intervals are identical to the values listed in Supplementary Table 6.

even accounting for BMI and total body fat percentage⁴¹. In light of the reported inverse relationships between abdominal body fat and pulmonary function^{30,32}, the disproportionate accumulation of abdominal and visceral body fat among males may explain the greater decrease in SpO_2 with each incremental increase in BMI.

The significant sex-dependent trends for SpO_2 vs. age observed in our data (Fig. 5b, f) have not been reported previously among healthy cohorts. However, some pathological lung conditions such as asthma, COPD and pulmonary hypertension display prevalence trends that vary with sex, potentially mediated through the influence of sex hormones on lung function⁴². The transition from regular menstrual status to post-menopause is associated with acceleration of age-related decline in lung function, as quantified by lung capacity metrics such as forced vital capacity⁴³. Additionally, sex-dependent differences in age-related trends have been reported for some cardiovascular metrics including blood pressure^{44,45}.

In conjunction with the significant difference in age-related SpO_2 trends between males and females, it is also important to note that the constant terms do not differ statistically between the sexes. Controlling for altitude and BMI, sex-specific differences are small or negligible for young individuals, although with advancing age mean SpO_2 declines faster for females than males. This effect can be observed visually in Fig. 1d, which overlays male and female mean 24-h SpO_2 profiles for moderate-BMI, low-altitude subject groups of two different age strata (20–30 years and 60–70 years). In the younger age group males and females present nearly equal mean SpO_2 across all hours of the day, however for older ages the SpO_2 profiles diverge and females exhibit lower SpO_2 across all hours.

The decline in SpO_2 with increasing altitude is well-established, and occurs as a direct result of the reduced oxygen partial pressure in the ambient environment. Because of the nonlinear (though monotonic) relationship between altitude and mean atmospheric pressure⁴⁶, and the sigmoid shape of the oxygen-hemoglobin dissociation curve⁴⁷, the theoretical trend for arterial oxygen saturation with altitude is not expected to be perfectly linear. However, significant deviation from a consistent linear trend only occurs at high altitudes (>2500 m)⁴⁸, and therefore for altitude range evaluated in our data set a linear approximation is adequate.

Given the optical basis for the function of pulse oximeter devices, which employ both infrared and visible wavelengths of light, many researchers and clinicians have raised valid concerns regarding the accuracy of pulse oximetry measurements across the full spectrum of human skin tone. Three recent studies utilizing large hospital-gathered data sets consisting of

opportunistic paired SpO_2 and arterial blood gas measurements have reported significant differences in SpO_2 measurement accuracy depending on patient race and ethnicity at low oxygen saturation values^{49–52}. These inaccuracies among in-hospital SpO_2 measurements disproportionately impact patients of non-White race/ethnicity⁵⁰, particularly Black individuals^{49,51,52}.

On the data set reported here, stratified analysis according to self-reported race/ethnicity (Fig. 6 and Supplementary Table 6) does not indicate the presence of any significant or meaningful systematic bias in SpO_2 measurements between race/ethnicity groups. For both $dSpO_2$ and $nSpO_2$, regression models fit to subjects of each race/ethnicity group yield constant terms with no significant differences between groups (Fig. 6a, e). Additionally, for regression models incorporating categorical variables encoding each race/ethnicity group fit to female subjects, male subjects, and the full subject cohort (rightmost four columns of Table 3 and Supplementary Table 5, race/ethnicity coefficients correspond to differences smaller than $\pm 0.15\%$ saturation between White and non-White subject groups in our dataset. Combined, this suggests the absence of a clinically meaningful SpO_2 measurement bias with skin tone over the range of saturation values collected in this study. However, because this data set consists of nominally healthy individuals outside of clinical settings, the range of measured SpO_2 values is heavily weighted toward non-hypoxic conditions. Just 2.5% of all collected SpO_2 values fall below 90% saturation, and 0.29% fall below 85% saturation (Fig. 7). Therefore using this data set we are not able to confirm or refute the systematic race/ethnicity differences reported from clinical SpO_2 data sets that include hypoxic values^{49–51}.

For further inspection of differences in mean SpO_2 according to race/ethnicity, we also compared $dSpO_2$ and $nSpO_2$ distributions by race/ethnicity group after linear adjustment all individual data points (using sex-specific regression model fits) to correspond to subject age of 40 years, BMI of 25.0, and sea level home altitude. The resulting distributions show no statistically significant differences between race/ethnicity groups based on two-sample Kolmogorov–Smirnov tests, either over the full SpO_2 range or if the distributions are clipped at 94% saturation to emphasize the hypoxic SpO_2 range. An example comparison of adjusted $nSpO_2$ distributions for Black and White subjects is shown in Supplementary Fig. 7.

This study has several important limitations. Although the Apple Heart & Movement Study represents a large total subject pool, it contains significant demographic imbalances as illustrated in Fig. 8d and Table 4. For example, 53% of the cohort used in the analysis reported here is White and male. Additionally all subject metadata including age, body measurements, geographic location

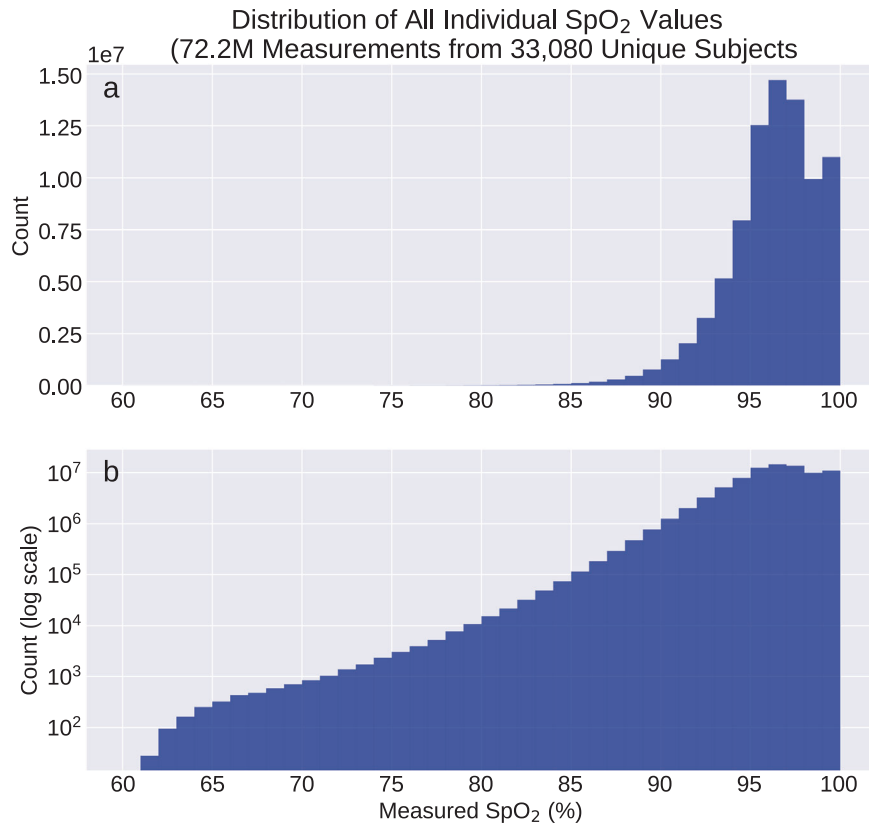


Fig. 7 Histograms of all individual SpO₂ values collected from the full subject cohort. **a** Distribution counts shown with linear y-scale. **b** Distribution counts shown with logarithmic y-scale. The two histograms represent identical data, but with differing y-scales to enable useful visualization of the value distribution for SpO₂ < 85%.

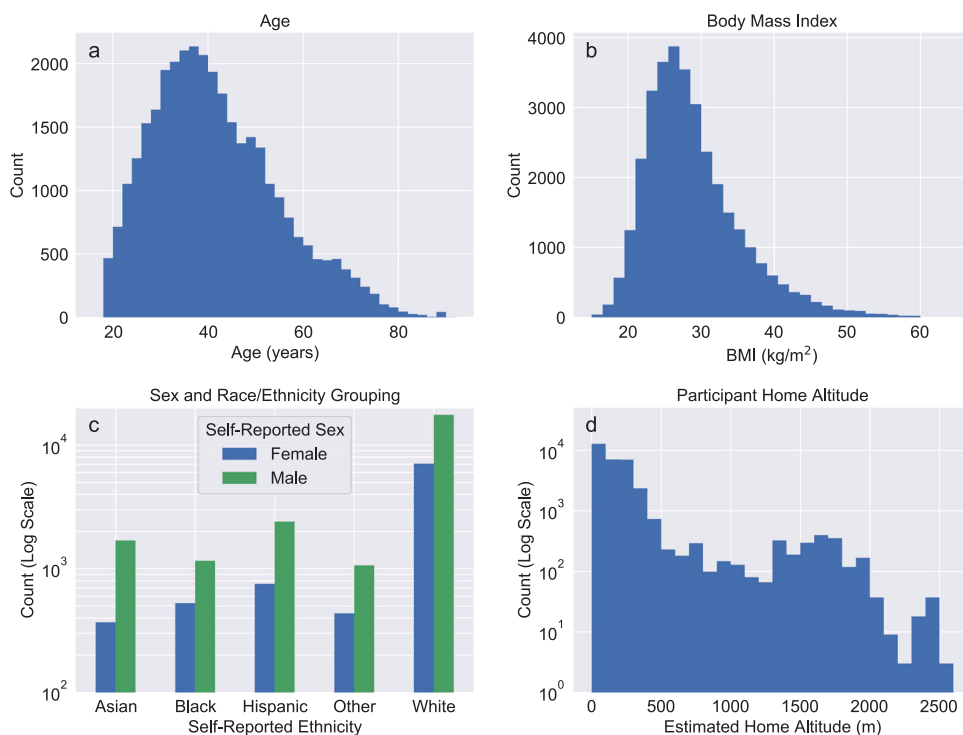


Fig. 8 Demographic variable distributions for all subjects used in the analysis. **a** Age, **b** BMI, **c** sex and race/ethnicity, **d** home altitude. Note that for age and BMI the y-axis representing subject counts uses a linear scale, while for sex and race/ethnicity groups and estimated home altitude the y-axis uses logarithmic scale for clarity.

(from which elevation and barometric pressure are inferred), sex, and race/ethnicity have been provided by subject self-report without independent verification.

This study did not exclude any subjects based upon cardiovascular or pulmonary disease risk factors, behavior (including alcohol and smoking habits), or self-reported chronic health conditions that may significantly impact blood oxygen saturation (such as COPD, emphysema, sleep apnea, and heart failure). However, regression modeling on subjects stratified according to self-reported health conditions and smoking habits indicates that systematic decline in SpO₂ with Age and BMI occurs at rates that are similar for healthy lifetime nonsmokers as well as individuals who smoke or have chronic cardiopulmonary conditions (results summarized in Supplementary Note 5, Supplementary Fig. 5, and Supplementary Table 11).

The study period also occurred in the midst of the COVID-19 pandemic (spanning the timeframe when vaccination became widely available in the US), during which an unknown fraction of the study population may have experienced acute respiratory infection. As such, the aggregated data inevitably includes some measurements collected under pathological conditions and this may influence the resulting population-scale observations and statistical models. Additionally, reducing the data collection window to a maximum of 30 consecutive calendar days per subject did not meaningfully impact the downstream regression modeling results (results summarized in Supplementary Note 4, Supplementary Fig. 4, and Supplementary Table 10).

All data in the study was collected in uncontrolled naturalistic conditions, and therefore contains a large variety of unknown measurement contexts and use conditions which may influence the measured SpO₂ values. Additionally, the grouping of measurements into nocturnal vs. daytime average values is determined by referencing against local clock time, as opposed to grouping according to subject-specific physiological measures such as sleep or activity state. This grouping likely introduces a mix of both awake and asleep measurements into each subject's dSpO₂ and nSpO₂ values. However, fitting and comparing linear model coefficients for individual clock hours does not reveal significant variability between adjacent hours, but rather a smooth circadian variation for each coefficient value (results shown in Supplementary Fig. 3). Additional analysis utilizing sleep tracking data from a subset of subjects to align SpO₂ measurements with circadian sleep/wake schedule did not meaningfully impact the downstream regression modeling results (results summarized in Supplementary Note 3, Supplementary Figs. 1 and 2, and Supplementary Table 9).

Lastly, because the AppleWatch Series 6 sensor is not a CO-oximeter it is unable to measure or account for the presence of non-oxygen-carrying dyshemoglobin compounds such as carboxyhemoglobin (which may be increased due to use of cigarettes and exposure to other smoke sources), sulfhemoglobin, and methemoglobin.

METHODS

Data collection

This study examined data from the Apple Heart and Movement Study, an ongoing research study beginning November 14, 2019 conducted in partnership with American Heart Association and Brigham and Women's Hospital that was designed to explore the links between physical activity and cardiovascular health. Study participants were all Apple Watch users at least 18 years old residing in the United States, and provided informed consent electronically in the Apple Research app. The study was approved by the Advarra Central Institutional Review Board, and registered to ClinicalTrials.gov (ClinicalTrials.gov Identifier: NCT04198194)⁵³.

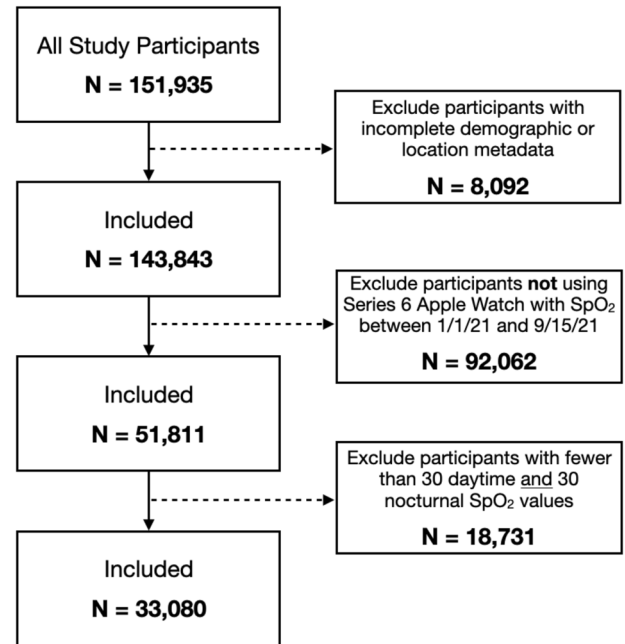


Fig. 9 Subject inclusion/exclusion criteria flowchart.

All data collection, both raw measurements and metadata, was accomplished using the using the Apple Research app.

Subjects were selected for inclusion in downstream analysis based on use of a Series 6 Apple Watch and contribution of sufficient SpO₂ measurements during the study period as described in the flowchart in Fig. 9. Subject demographic distributions including age, body mass index, estimated home altitude, and self-reported race and ethnicity are summarized in Fig. 8. Geographic information was based on zip (postal) code, with 3-5 zip code digits available depending on total participant count in that location (for privacy purposes, zip codes containing few subjects were reported with the trailing two digits redacted). Approximate home altitude was determined by associating the zip code information with USGS mean surface elevation in the corresponding geographic area. Due to comparatively small numbers of individuals self-reporting ethnicity of "American Indian or Alaskan Native," "Middle Eastern or North African," "Native Hawaiian or other Pacific Islander," and "None of these fully describes me," these subjects were combined into a single race/ethnicity group (Other) when used for downstream subgroup and stratified analysis. Body mass index was determined from height and weight, and mean barometric pressure was calculated from home altitude using the reference NOAA Pressure Altitude equation⁴⁶. Tabulated summary statistics and statistical comparisons are shown in Table 4.

All individual SpO₂ measurements from Series 6 Watches collected between January 1, 2021 and September 15, 2021 were aggregated from active study participants, along with self-reported demographic information. Blood oxygen saturation values were measured using the Apple-developed SpO₂ sensor available on some Apple Watch models (only data from Apple Watch Series 6 devices is utilized in the present study). SpO₂ values were acquired both on-demand (initiated by the watch wearer) as well as passively via background measurements attempted automatically under low-motion conditions at roughly 30-min cadence. Histograms of all individual SpO₂ values (ranging from 60 to 100% saturation with integer values) collected from the full study cohort are shown in Fig. 7. The Apple Watch SpO₂ measurement accuracy compared against reference clinical fingertip pulse oximeters has been reported elsewhere for healthy

Table 5. Summary of models employed in linear regression analysis.

Model name	Covariates	Model usage
M_{Age}	Age (years)	Comparison with low-altitude univariate SaO ₂ model (Crapo, et al. ³)
M_{Ref}	Age (years) Height (cm) Weight (kg) Barometric pressure (mmHg) Sex (categorical)	Comparison with reference SaO ₂ model (Crapo, et al. ³)
M_1	Age-40 (years) BMI-25 (kg/m ²) Home altitude (km) Sex (categorical) Race/ethnicity (categorical)	Proposed full-cohort SpO ₂ linear model
$M_{1,sex}$	Age-40 (years) BMI-25 (kg/m ²) Home altitude (km) Race/ethnicity (categorical)	Sex-stratified analysis
$M_{1,race-ethn.}$	Age-40 (years) BMI-25 (kg/m ²) Home altitude (km) Sex (categorical)	Race/ethnicity-stratified analysis

$M_{1,sex}$ differs from M_1 only by the omission of the categorical variable encoding sex. $M_{1,race-ethn.}$ differs from M_1 only by the omission of the categorical variables encoding race/ethnicity.

subject cohorts ($N = 265$ subjects, mean bias -0.23% , 95% limits of agreement -3.49% to 3.04% compared with Nellcor PM10N Oximeter reference⁵⁴) and cohorts enriched with cardiopulmonary disease ($N = 100$ subjects, mean bias 0.8% , 95% limits of agreement -2.7% to 4.1% compared with Mobil POD-2 Finger Oximeter and Multilaser OX-06 Oximeter references⁵⁵).

Individual SpO₂ values were labeled with timestamps corresponding to wall clock time in the subject's local time zone. All downstream analysis utilized data from subjects contributing at least 30 individual SpO₂ measurements during typical mid-sleep hours (local wall clock time 01:00–04:59) as well as at least 30 individual SpO₂ measurements during typical awake daytime hours (local wall clock time 11:00–18:59). For subjects satisfying these selection criteria (Fig. 9) all SpO₂ measurements collected during the study period were retained, with no outlier rejection, thresholding, filtering, or other removal of individual SpO₂ values. This data aggregation yielded 33,080 unique subjects contributing over 72.2 million individual SpO₂ values (median 1772 values/subject) spanning all hours of the day. A complete dataset for each subject consisted of mean daytime and nocturnal SpO₂, approximate home altitude inferred from zip code information, and self-reported age, assigned sex, height, weight, and race/ethnicity.

Data processing

Individual SpO₂ values from each subject were grouped and averaged by hour of the day, yielding a single 24-h mean SpO₂ profile per subject, irrespective of the subject's total number of

collected SpO₂ measurements or their hourly distribution throughout the day. Subject 24-h profiles were then averaged over either the full cohort or various subject groups (for example subjects stratified by decade of age or BMI category). The 24-h SpO₂ profile mean and standard deviation for the general cohort is shown in Fig. 2, and 24-h SpO₂ profile means and 99.5% confidence interval profiles for subject groups stratified by age, BMI, home altitude, and sex are shown in Fig. 1. This method for aggregating hourly SpO₂ values for the full cohort and stratified groups minimizes bias due to the number of individual measurements per subject, and has been reported in prior literature for circadian analysis of blood pressure profiles stratified by various demographic variables⁴⁵.

Per-subject mean daytime oxygen saturation (dSpO₂) and mean nocturnal oxygen saturation (nSpO₂) were calculated for each individual by averaging all SpO₂ values occurring between 11:00 and 18:59 local clock time, and 01:00–04:59 local clock time, respectively. The hourly time ranges used to define dSpO₂ and nSpO₂ were chosen prior to performing downstream statistical analysis on these metrics. Mean day–night oxygen saturation difference (dnΔSpO₂) for each individual was determined from the difference between these two metrics (dSpO₂ – nSpO₂), with positive values of dnΔSpO₂ corresponding to lower average blood oxygen saturation overnight than during the daytime. Full-cohort distributions of dSpO₂, nSpO₂, and dnΔSpO₂ are shown in Fig. 3.

Statistical analysis

Plotting and data visualization were performed using the Python packages Seaborn⁵⁶ (version 0.11.0) and Matplotlib⁵⁷ (version 3.2.2). Ordinary least squares linear regression modeling (OLS) was performed using the Python statsmodels module⁵⁸ (version 0.11.1) to quantify systematic factors impacting measured blood oxygen saturation at the population level. Dependent variables consisted of dSpO₂ and nSpO₂ separately. Various sets of independent variables were used for fitting linear regression models, with all reported models summarized in Table 5.

Analysis of sources of variation in daytime and nocturnal SpO₂ was accomplished by first calculating dSpO₂ and nSpO₂ for each subject on a date-by-date basis, then performing nested one-way ANOVA and variance components analysis (VCA) utilizing mixed-effects modeling as reported in the Supplementary Materials (Supplementary Note 1 and Supplementary Tables 3 and 4). For both daytime and nocturnal SpO₂, nested ANOVA and VCA both support the conclusion that the predominant contributor to daily measurement variance is subject-to-subject differences.

For direct comparison with the arterial oxygen saturation reference equation reported by Crapo et al.³, dSpO₂ and nSpO₂ were modeled using a combination of age, height, weight, assigned sex and inferred barometric pressure (estimated from home altitude). This reference model employing height and weight separately in place of BMI, and barometric pressure in place of home altitude, is referred to as M_{Ref} in subsequent discussion. For subjects residing at low altitude (below the dataset median of 155m) we fit a simple univariate model (M_{Age}) for dSpO₂ using only age as the independent variable, for comparison against the univariate regression model reported by Crapo et al. for low-altitude measurements³.

For additional full-cohort analysis we fit dSpO₂ and nSpO₂ using model M_1 , which employed linear terms for the following covariates: age, BMI, estimated home altitude, assigned sex (categorically encoded using 1 corresponding to male sex and 0 corresponding to female sex), and self-reported race/ethnicity group (categorically encoded using dummy variables, with 'White' race/ethnicity used as the reference category based on greatest subject count in this subject group). Quadratic terms for age, BMI and altitude were evaluated but did not produce models with meaningfully different goodness of fit metrics compared to

models using only linear terms, and so were not utilized for further analysis. For all fits using model M_1 , $M_{1,sex}$ and $M_{1,race-ethn.}$ the age and BMI covariates were centered at 40 years and 25.0 BMI points, respectively. Estimated home altitude values were used uncentered. The fitted constant terms therefore represent the predicted mean SpO₂ for an individual residing at sea level with age 40 and BMI of 25.0 points.

In order to evaluate the presence of systematic factors impacting measured SpO₂ as a function of subject sex, race or ethnicity, we performed the following analysis across subject groups using dSpO₂ and nSpO₂ as dependent variables:

- Model coefficients and confidence intervals corresponding to sex and race/ethnicity variables were examined, for the M_1 model fit to the full subject cohort.
- Stratified regression models were fit separately for male and female participants using model $M_{1,sex}$ and the resulting coefficients and confidence intervals were compared between these models.
- Stratified regression models were fit separately for participants in each race/ethnicity group using model $M_{1,race-ethn.}$ and the resulting coefficients and confidence intervals compared between models.

Additional regression models incorporating linear interaction terms for sex and race/ethnicity were investigated, but yielded either inferior goodness of fit metrics (compared with model M_1) or produced results numerically equivalent to the stratified regression models $M_{1,sex}$ and $M_{1,race-ethn.}$ Details of these alternative investigated models are provided in Supplementary Note 2 and Supplementary Tables 7 and 8.

In accordance with recent recommendations regarding use of p values in statistical analysis⁵⁹, we have used a threshold of $p < 0.005$ (rather than $p < 0.05$) to determine statistical significance. Correspondingly, we report uncertainty for fitted model coefficients using 99.5% confidence intervals, and all plotted error bars correspond to 99.5% confidence interval. For the grouped circadian SpO₂ profiles shown in Fig. 1), error whiskers represent 2.81 times the standard error of the mean (SEM) to reflect 99.5% confidence interval. All p values were calculated using the SciPy stats package⁶⁰ (version 1.5.0). p Values reported for linear regression coefficients correspond to two-sided t tests under the null hypothesis that the coefficient is equal to zero. In stratified analysis, p values reported for comparing coefficients between separate linear regression models fit to independent data subsets (for example data from females vs. males) were determined using Welch's unequal variances t test, under the null hypothesis that the two coefficients are equal. For race/ethnicity stratified analysis, when comparing coefficients between models we utilized a Bonferroni-corrected p value threshold of < 0.0005 to account for multiple pairwise comparisons.

Reporting summary

Further information on research design is available in the Nature Research Reporting Summary linked to this article.

DATA AVAILABILITY

The aggregated data that support the findings of this study can be made available on request from the corresponding author (M.O.). Request for data will be evaluated and responded to in a manner consistent with the specific language in the study protocol and informed consent form.

CODE AVAILABILITY

Code for all data analyses and statistical modeling was written in Python 3.6. This code may be available upon request from the corresponding author (M.O.). Requests for code will be evaluated and responded to in a manner consistent with policies intended to protect participant confidentiality and language in the study protocol and informed consent form.

Received: 25 June 2022; Accepted: 24 May 2023;

Published online: 27 July 2023

REFERENCES

1. Neff, T. A. Routine oximetry: a fifth vital sign? *Chest* **94**, 227 (1988).
2. Mower, W. R., Sachs, C., Nicklin, E. L. & Baraff, L. J. Pulse oximetry as a fifth pediatric vital sign. *Pediatrics* **99**, 681–686 (1997).
3. Crapo, R. O., Jensen, R. L., Hegewald, M. & Tashkin, D. P. Arterial blood gas reference values for sea level and an altitude of 1,400 meters. *Am. J. Respir. Crit. Care Med.* **160**, 1525–1531 (1999).
4. Vold, M. L., Aasebø, U., Hjalmsen, A. & Melbye, H. Predictors of oxygen saturation $\leq 95\%$ in a cross-sectional population based survey. *Respir. Med.* **106**, 1551–1558 (2012).
5. Witting, D. W. & Scharf, S. M. Diagnostic room-air pulse oximetry: effects of smoking, race, and sex. *Am. J. Emerg. Med.* **26**, 131–136 (2008).
6. Vold, M. L., Aasebø, U. & Melbye, H. Low fev₁, smoking history, and obesity are factors associated with oxygen saturation decrease in an adult population cohort. *Int. J. Chron. Obstruct. Pulm. Dis.* **9**, 1225 (2014).
7. Kapur, V. K. et al. Obesity is associated with a lower resting oxygen saturation in the ambulatory elderly: results from the cardiovascular health study. *Respir. Care* **58**, 831–837 (2013).
8. Dockery, D. W., Pope, C., Kanner, R. E., Villegas, G. M. & Schwartz, J. Daily changes in oxygen saturation and pulse rate associated with particulate air pollution and barometric pressure. *Res. Rep. Health Eff. Inst.* 1–19 (1999).
9. Pope, C. A. I., Dockery, D. W., Kanner, R. E., Villegas, G. M. & Schwartz, J. Oxygen saturation, pulse rate, and particulate air pollution: a daily time-series panel study. *Am. J. Respir. Crit. Care Med.* **159**, 365–372 (1999).
10. Ceylan, B., Khorshid, L., Güneş, Ü. Y. & Zaybak, A. Evaluation of oxygen saturation values in different body positions in healthy individuals. *J. Clin. Nurs.* **25**, 1095–1100 (2016).
11. Levental, S. et al. Sex-linked difference in blood oxygen saturation. *Clin. Respir. J.* **12**, 1900–1904 (2018).
12. Smith, G. B. et al. SpO₂ values in acute medical admissions breathing air—implications for the british thoracic society guideline for emergency oxygen use in adult patients? *Resuscitation* **83**, 1201–1205 (2012).
13. Natsios, G. et al. Age, body mass index, and daytime and nocturnal hypoxia as predictors of hypertension in patients with obstructive sleep apnea. *J. Clin. Hypertens.* **18**, 146–152 (2016).
14. Vold, M. L., Aasebø, U., Wilsgaard, T. & Melbye, H. Low oxygen saturation and mortality in an adult cohort: the Tromsø study. *BMC Pulm. Med.* **15**, 1–12 (2015).
15. Dalbak, L. G. et al. Impaired left ventricular filling is associated with decreased pulse oximetry values. *Scand. Cardiovasc. J.* **52**, 211–217 (2018).
16. Kishimoto, A., Tochikubo, O. & Ohshige, K. Relation between nocturnal arterial oxygen desaturation and morning blood pressure. *Clin. Exp. Hypertens.* **29**, 51–60 (2007).
17. Baguet, J.-P. et al. The severity of oxygen desaturation is predictive of carotid wall thickening and plaque occurrence. *Chest* **128**, 3407–3412 (2005).
18. Gunnarsson, S. I. et al. Minimal nocturnal oxygen saturation predicts future subclinical carotid atherosclerosis: the wisconsin sleep cohort. *J. Sleep Res.* **24**, 680–686 (2015).
19. Klæstrup, E. et al. Reference intervals and age and gender dependency for arterial blood gases and electrolytes in adults. *Clin. Chem. Lab. Med.* **49**, 1495–1500 (2011).
20. Perez-Padilla, R. et al. Prevalence of oxygen desaturation and use of oxygen at home in adults at sea level and at moderate altitude. *Eur. Respir. J.* **27**, 594–599 (2006).
21. Vargas, M. H., Rodríguez-Godínez, I., Arias-Gómez, J. & Furuya, M. E. Y. Circadian variability of pulse oximetry in healthy children under the age of 7. *Arch. Bronconeumol. (Engl. Ed.)* **48**, 202–206 (2012).
22. Cristancho, E., Riveros, A., Sánchez, A., Peñuela, O. & Böning, D. Diurnal changes of arterial oxygen saturation and erythropoietin concentration in male and female highlanders. *Physiol. Rep.* **4**, e12901 (2016).
23. Spengler, C. M. & Shea, S. A. Endogenous circadian rhythm of pulmonary function in healthy humans. *Am. J. Respir. Crit. Care Med.* **162**, 1038–1046 (2000).
24. Medarov, B. I., Pavlov, V. A. & Rossoff, L. Diurnal variations in human pulmonary function. *Int. J. Clin. Exp. Med.* **1**, 267 (2008).
25. Marti, C. & Ulmer, W. Absence of effect of the body position on arterial blood gases. *Respiration* **43**, 41–44 (1982).
26. Skloot, G. S. The effects of aging on lung structure and function. *Clin. Geriatr. Med.* **33**, 447–457 (2017).
27. Vaz Fragoso, C. A. & Gill, T. M. Respiratory impairment and the aging lung: a novel paradigm for assessing pulmonary function. *J. Gerontol. Ser. A Biomed. Sci. Med. Sci.* **67**, 264–275 (2012).
28. Cardus, J. et al. Increase in pulmonary ventilation-perfusion inequality with age in healthy individuals. *Am. J. Respir. Crit. Care Med.* **156**, 648–653 (1997).

29. Neufeld, O., Smith, J. R. & Goldman, S. Arterial oxygen tension in relation to age in hospital subjects. *J. Am. Geriatr. Soc.* **21**, 4–9 (1973).
30. Littleton, S. W. & Tulaimat, A. The effects of obesity on lung volumes and oxygenation. *Respir. Med.* **124**, 15–20 (2017).
31. Saliman, J. A. et al. Pulmonary function in the morbidly obese. *Surg. Obes. Relat. Dis.* **4**, 632–639 (2008).
32. Zavorsky, G. S. et al. Waist-to-hip ratio is associated with pulmonary gas exchange in the morbidly obese. *Chest* **131**, 362–367 (2007).
33. Zavorsky, G. & Hoffman, S. Pulmonary gas exchange in the morbidly obese. *Obes. Rev.* **9**, 326–339 (2008).
34. Jenkins, S. & Moxham, J. The effects of mild obesity on lung function. *Respir. Med.* **85**, 309–311 (1991).
35. Littleton, S. W. Impact of obesity on respiratory function. *Respirology* **17**, 43–49 (2012).
36. Jones, R. L. & Nzekwu, M.-M. U. The effects of body mass index on lung volumes. *Chest* **130**, 827–833 (2006).
37. Chen, Y.-Y. et al. Body fat percentage in relation to lung function in individuals with normal weight obesity. *Sci. Rep.* **9**, 1–7 (2019).
38. Gol, R. M. & Rafrat, M. Association between abdominal obesity and pulmonary function in apparently healthy adults: a systematic review. *Obes. Res. Clin. Pract.* **15**, 415–424 (2021).
39. Rutting, S. et al. Obesity alters the topographical distribution of ventilation and the regional response to bronchoconstriction. *J. Appl. Physiol.* **128**, 168–177 (2020).
40. Malik, V., Smith, D. & Lee-Chiong, T. Respiratory physiology during sleep. *Sleep Med. Clin.* **7**, 497–505 (2012).
41. Tchernof, A. & Després, J.-P. Pathophysiology of human visceral obesity: an update. *Physiol. Rev.* **93**, 359–404 (2013).
42. Townsend, E. A., Miller, V. M. & Prakash, Y. Sex differences and sex steroids in lung health and disease. *Endocr. Rev.* **33**, 1–47 (2012).
43. Triebner, K. et al. Menopause is associated with accelerated lung function decline. *Am. J. Respir. Crit. Care Med.* **195**, 1058–1065 (2017).
44. Ji, H. et al. Sex differences in blood pressure trajectories over the life course. *JAMA Cardiol.* **5**, 255–262 (2020).
45. Mahdi, A., Watkinson, P., McManus, R. J. & Tarassenko, L. Circadian blood pressure variations computed from 1.7 million measurements in an acute hospital setting. *Am. J. Hypertens.* **32**, 1154–1161 (2019).
46. National Oceanic and Atmospheric Administration. Pressure altitude calculator. <https://www.weather.gov/media/epz/wxcalc/pressureAltitude.pdf> (2023).
47. Severinghaus, J. W. Simple, accurate equations for human blood O₂ dissociation computations. *J. Appl. Physiol.* **46**, 599–602 (1979).
48. Rojas-Camayo, J. et al. Reference values for oxygen saturation from sea level to the highest human habitation in the andes in acclimatised persons. *Thorax* **73**, 776–778 (2018).
49. Sjoding, M. W., Dickson, R. P., Iwashyna, T. J., Gay, S. E. & Valley, T. S. Racial bias in pulse oximetry measurement. *N. Engl. J. Med.* **383**, 2477–2478 (2020).
50. Wong, A.-K. I. et al. Analysis of discrepancies between pulse oximetry and arterial oxygen saturation measurements by race and ethnicity and association with organ dysfunction and mortality. *JAMA Netw. Open* **4**, e2131674 (2021).
51. Valbuena, V. S. et al. Racial bias in pulse oximetry measurement among patients about to undergo ECMO in 2019–2020, a retrospective cohort study. *Chest* **161**, 971–978 (2022).
52. Andrist, E., Nuppenau, M., Barbaro, R. P., Valley, T. S. & Sjoding, M. W. Association of race with pulse oximetry accuracy in hospitalized children. *JAMA Netw. Open* **5**, e224584 (2022).
53. Apple Heart and Movement Study. <http://clinicaltrials.gov/show/NCT04198194> (2023).
54. Spaccarotella, C. et al. Assessment of non-invasive measurements of oxygen saturation and heart rate with an apple smartwatch: comparison with a standard pulse oximeter. *J. Clin. Med.* **11**, 1467 (2022).
55. Pipek, L. Z., Nascimento, R. F. V., Acencio, M. M. P. & Teixeira, L. R. Comparison of SpO₂ and heart rate values on apple watch and conventional commercial oximeters devices in patients with lung disease. *Sci. Rep.* **11**, 1–7 (2021).
56. Waskom, M. L. seaborn: Statistical data visualization. *J. Open Source Softw.* **6**, 3021 (2021).
57. Hunter, J. D. Matplotlib: a 2D graphics environment. *Comput. Sci. Eng.* **9**, 90–95 (2007).
58. Seabold, S. & Perktold, J. statsmodels: Econometric and statistical modeling with python. In *9th Python in Science Conference* 92–96 (SCIPY, 2010).
59. Benjamin, D. J. & Berger, J. O. Three recommendations for improving the use of p-values. *Am. Stat.* **73**, 186–191 (2019).
60. Virtanen, P. et al. SciPy 1.0: fundamental algorithms for scientific computing in Python. *Nat. Methods* **17**, 261–272 (2020).

ACKNOWLEDGEMENTS

The authors acknowledge the important data contributions provided by all participants in the Apple Heart & Movement Study, without whom this research would not be possible. We also thank the following individuals for their thoughtful discussion, helpful guidance, and other valuable effort in support of this work: Marni Bartlett, David Tsay, Asha Chesnutt, Jen Block, Laura Rhodes, Paul Mannheimer, Mai Le, Mohsen Mollazadeh, Aditya Dua, Max Akhterov, Chris Brouse, and Angela Spillane. The Apple Heart & Movement Study receives funding from Apple, Inc. and the American Heart Association.

AUTHOR CONTRIBUTIONS

I.S. analyzed the data, interpreted the results, and drafted the manuscript. J.S. analyzed the data and interpreted the results. C.M. designed the study. M.O. was responsible for the critical revision and final approval of the manuscript.

COMPETING INTERESTS

I.S., J.S., and M.O. are employees of Apple, Inc. and own Apple, Inc. stock. C.M. received grant funding from the American Heart Association for this work.

ADDITIONAL INFORMATION

Supplementary information The online version contains supplementary material available at <https://doi.org/10.1038/s41746-023-00851-6>.

Correspondence and requests for materials should be addressed to Michael O'Reilly.

Reprints and permission information is available at <http://www.nature.com/reprints>

Publisher's note Springer Nature remains neutral with regard to jurisdictional claims in published maps and institutional affiliations.



Open Access This article is licensed under a Creative Commons Attribution 4.0 International License, which permits use, sharing, adaptation, distribution and reproduction in any medium or format, as long as you give appropriate credit to the original author(s) and the source, provide a link to the Creative Commons license, and indicate if changes were made. The images or other third party material in this article are included in the article's Creative Commons license, unless indicated otherwise in a credit line to the material. If material is not included in the article's Creative Commons license and your intended use is not permitted by statutory regulation or exceeds the permitted use, you will need to obtain permission directly from the copyright holder. To view a copy of this license, visit <http://creativecommons.org/licenses/by/4.0/>.

© The Author(s) 2023